Supplementary Information

Vapor-phase hydrothermal construction of defective MoS_2 for highly selective electrocatalytic hydrogenation of cinnamaldehyde

Tianxing Wu, *[a] Miaomiao Han*[b]

[a] Northwest Institute for Non-ferrous Metal Research, Xi'an, 710016, P. R. China

[b] School of Science, Huzhou University, Huzhou, 313000, P. R. China

*Corresponding author.

E-mail addresses: mybestteacher@163.com (T. Wu)

mmhan@zjhu.edu.cn (M. Han)

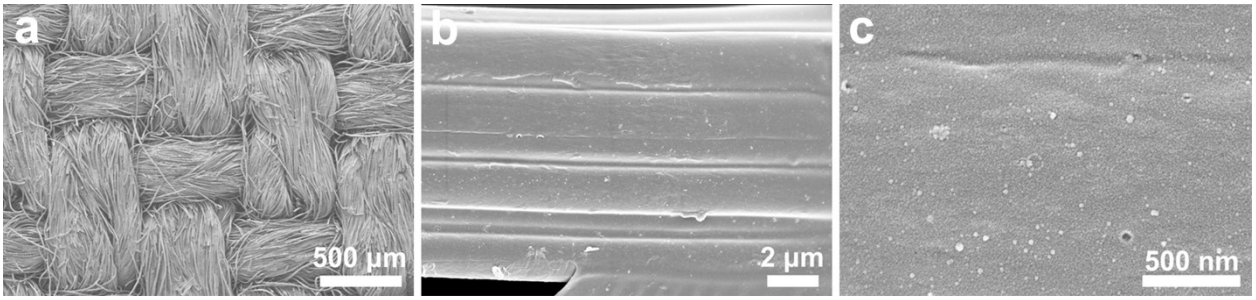

Fig. S1 SEM images of bare CFC.

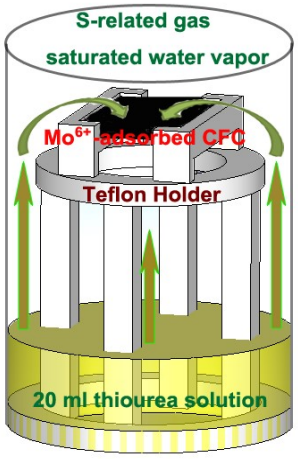

Fig. S2 Experimental set up of vapor-phase hydrothermal (VPH) method used in this work.

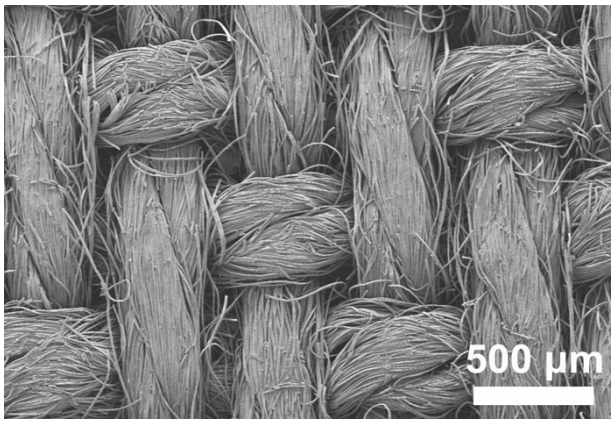

Fig. S3 Low-magnification SEM image of MoS_2/CFC.

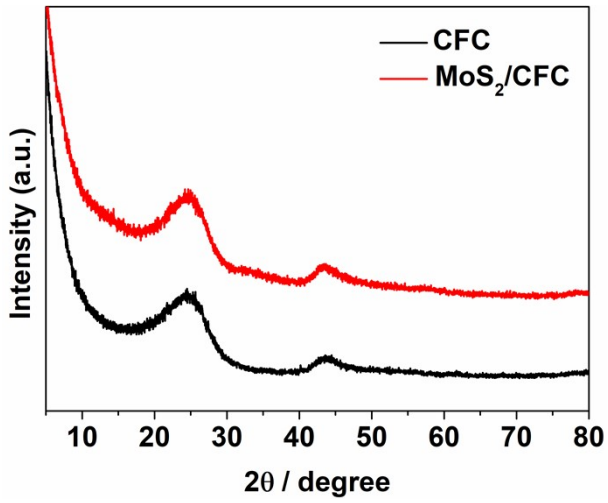

Fig. S4 XRD patterns of bare CFC and MoS_2/CFC.

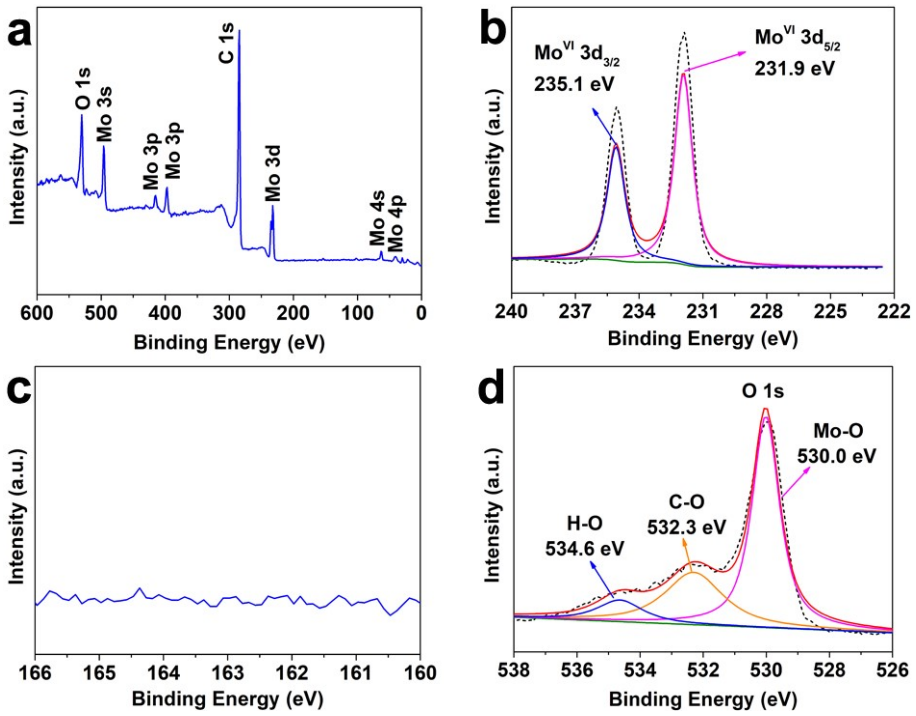

Fig. S5 (a) Surface survey XPS spectrum of Mo^{6+}-adsorbed CFC; High-resolution XPS spectra of (b) Mo 3d, (c) S 2p and (d) O 1s.

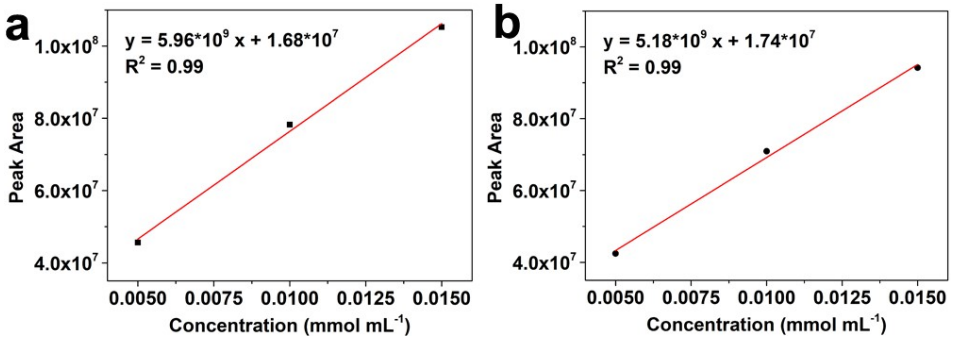

Fig. S6 Gas chromatograph spectrogram and the corresponding calibration curves of (a) CAL and (b) HCAL.

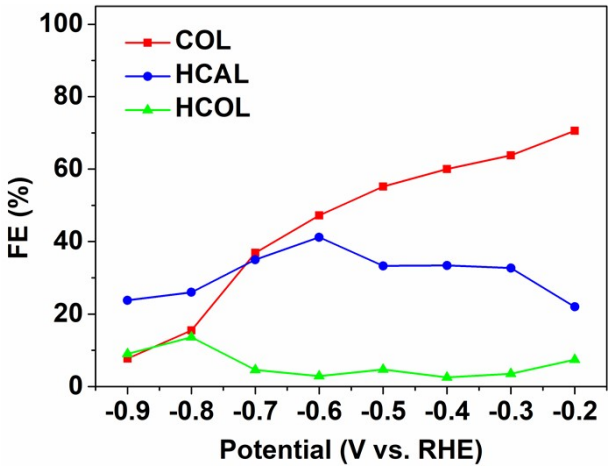

Fig. S7 The detailed FE values for COL, HCAL and HCOL.

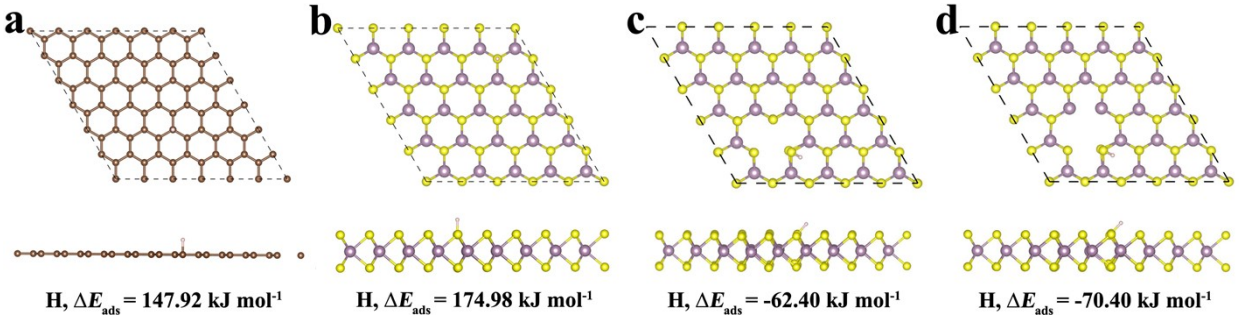

Fig. S8 Adsorption configurations and energies of H atom over (a) graphite carbon, (b) MoS_2 (002) surface, (c) MoS_2 (002) surface with Mo-vacancy, (d) MoS_2 (002) surface with Mo/S-vacancies (brown sphere: C, white sphere: H, yellow sphere: S, and purple sphere: Mo).

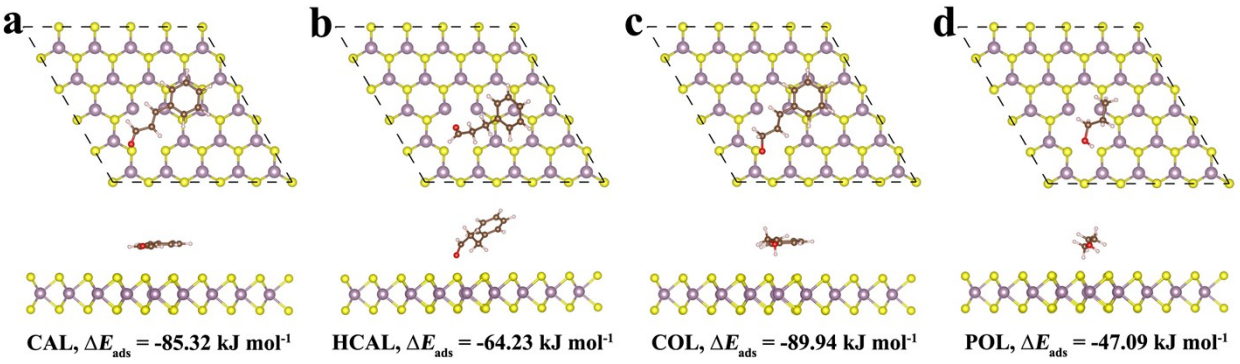

Fig. S9 Adsorption configurations and energies of different reacting species on MoS_2 (002) surface with Mo/S-vacancies (brown sphere: C, white sphere: H, red sphere: O, yellow sphere: S, and purple sphere: Mo).

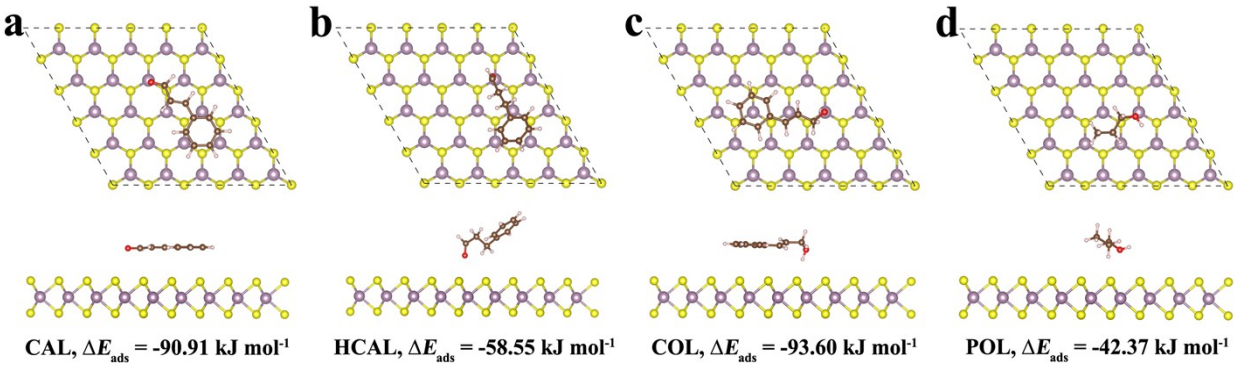

Fig. S10 Adsorption configurations and energies of different reacting species on bulk MoS_2 (002) surface (brown sphere: C, white sphere: H, red sphere: O, yellow sphere: S, and purple sphere: Mo).

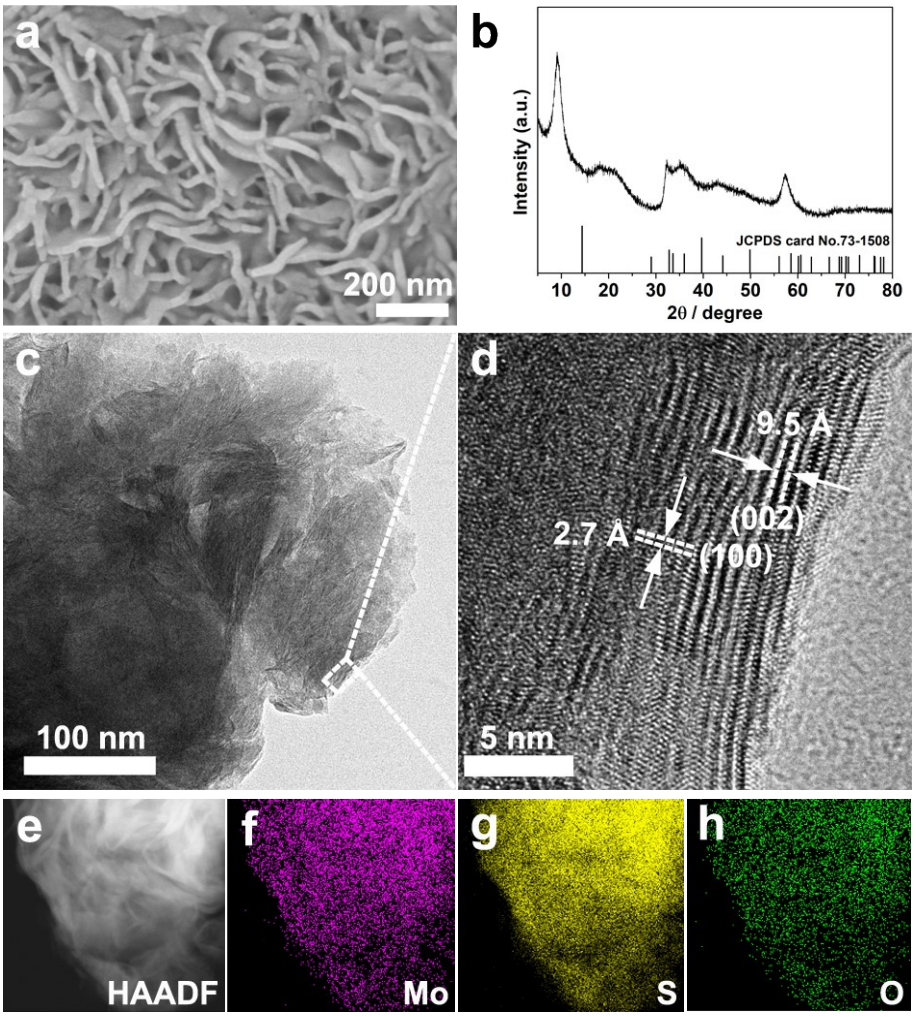

Fig. S11 Bulk MoS_2: (a) SEM image; (b) XRD pattern; (c) TEM image; (d) HRTEM image; (e) High-angle annular dark-field scanning transmission electron microscopy (HAADF-STEM) and (f-h) corresponding elemental mapping images.

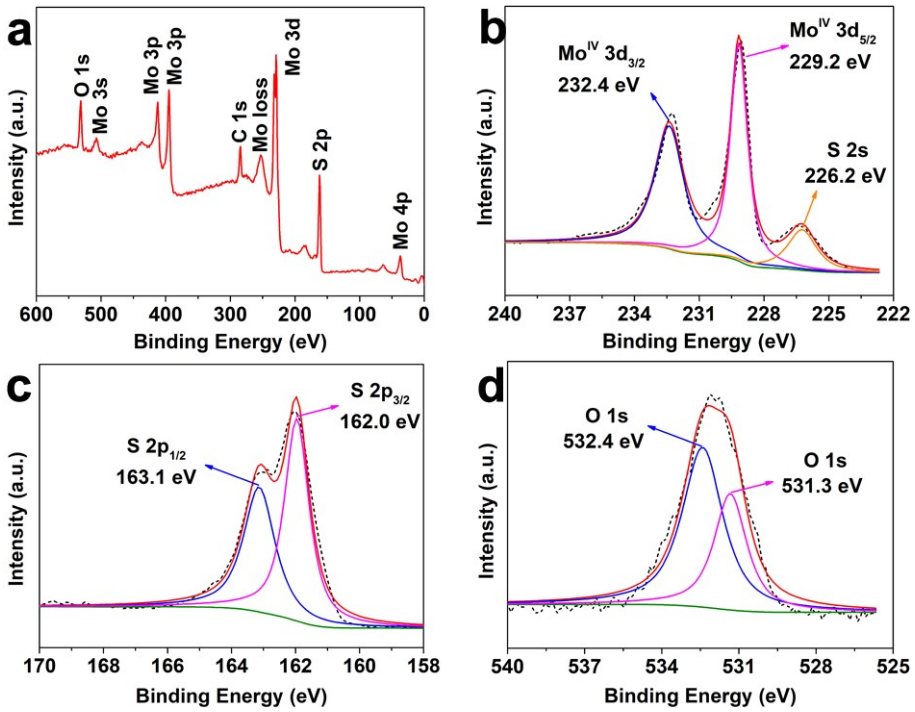

Fig. S12 Bulk MoS_2: (a) Surface survey XPS spectrum; High-resolution XPS spectra of (b) Mo 3d, (c) S 2p and (d) O 1s.

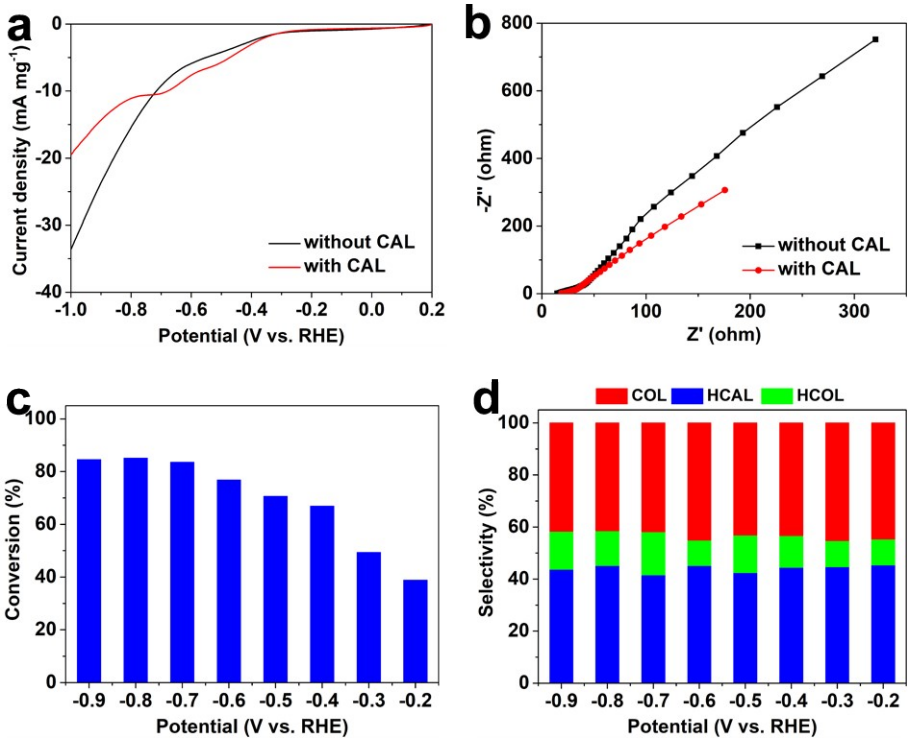

Fig. S13 (a) LSV curves and (b) EIS spectra of bulk MoS_2 in 0.1 M PBS electrolyte (pH=7.0) with and without CAL; (c) conversion; (d) selectivity.

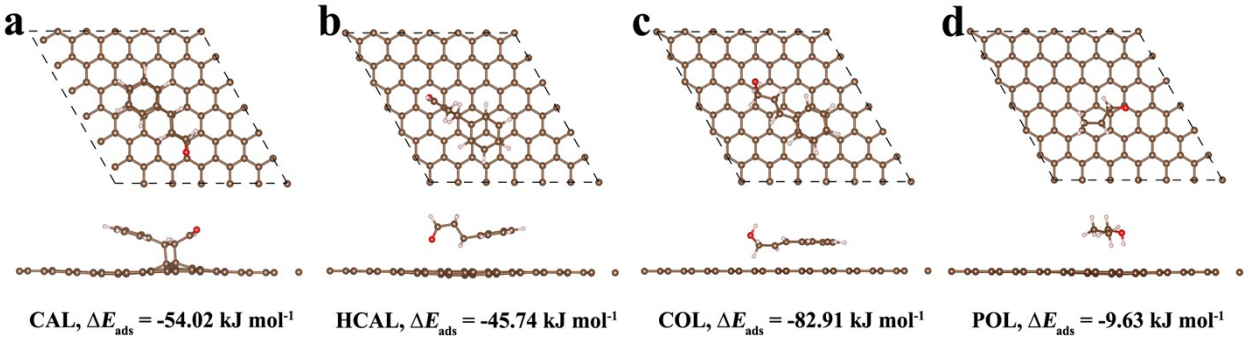

Fig. S14 Adsorption configurations and energies of different reacting species on graphite carbon (brown sphere: C, white sphere: H, red sphere: O).

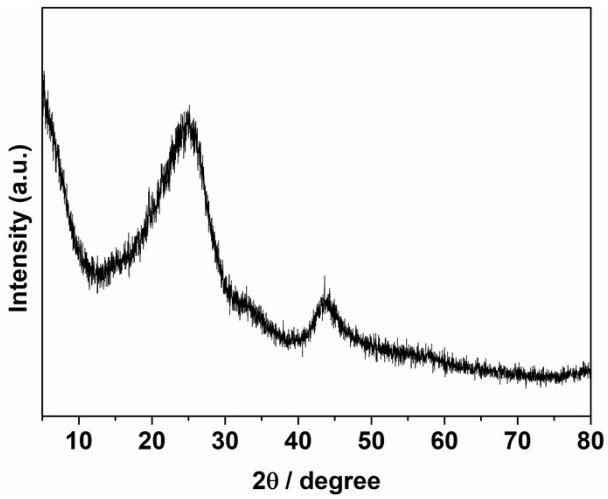

Fig. S15 XRD pattern of MoS_2/CFC after ECH measurements.

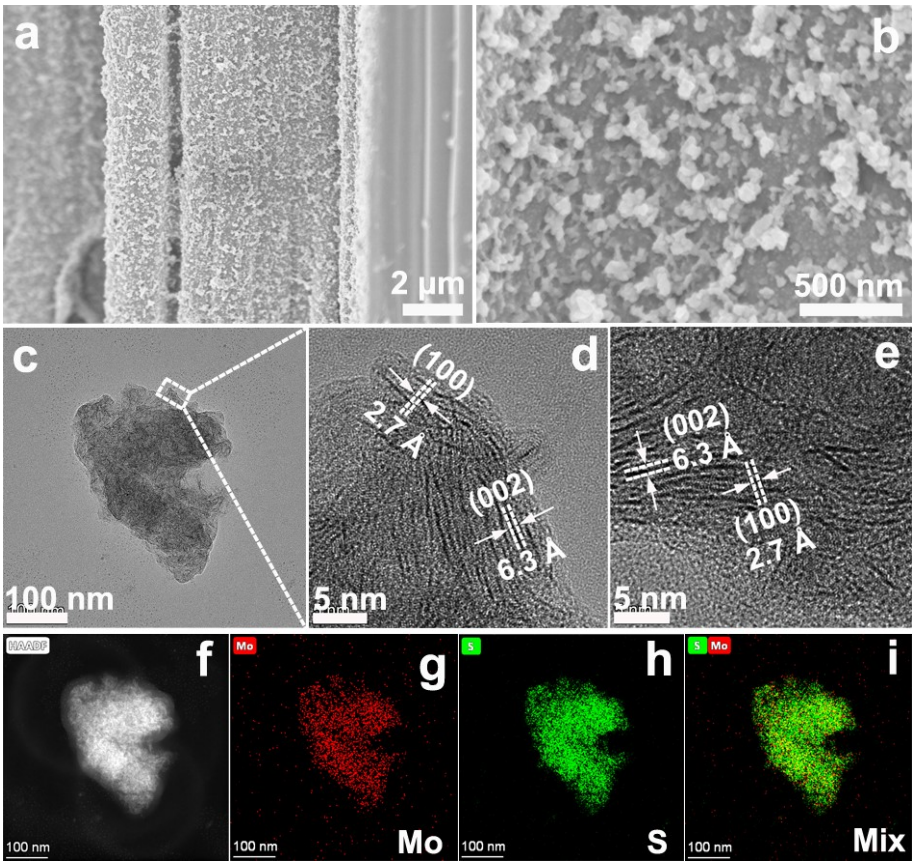

Fig. S16 MoS_2/CFC after ECH: (a) Low-magnification SEM image; (b) High-magnification SEM image; (c) TEM image; (d) HRTEM image; (e) High-angle annular dark-field scanning transmission electron microscopy (HAADF-STEM) and (f-i) corresponding elemental mapping images.

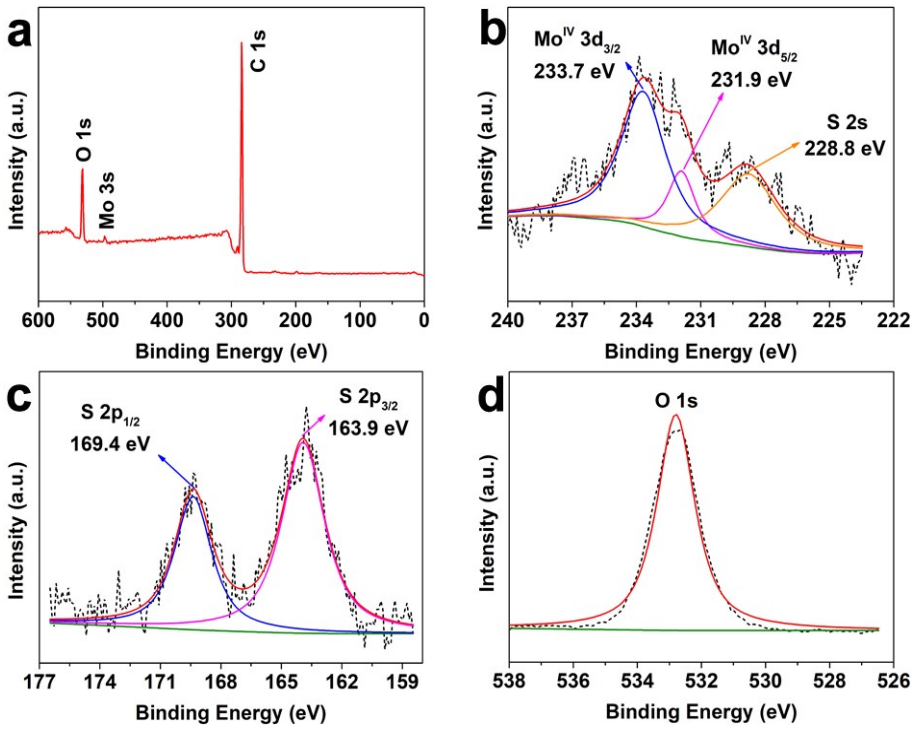

Fig. S17 MoS_2/CFC after ECH: (a) Surface survey XPS spectrum; High-resolution XPS spectra of (b) Mo 3d, (c) S 2p and (d) O 1s.

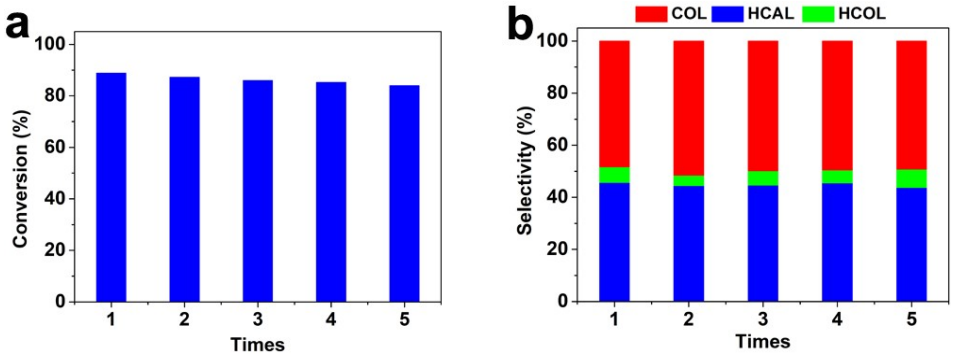

Fig. S18 The five consecutive cycling tests of MoS_2/CFC for electrocatalytic CAL hydrogenation under -0.7 V vs. RHE: (a) conversion, (b) selectivity.

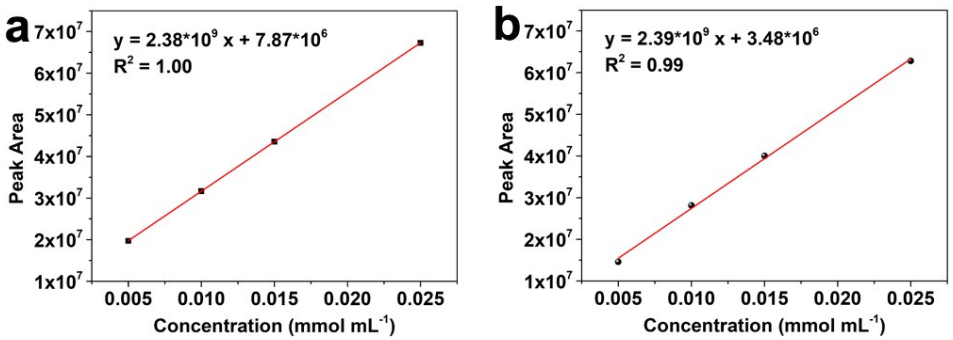

Fig. S19 Gas chromatograph spectrogram and the corresponding calibration curves of (a) FAL and (b) FOL.

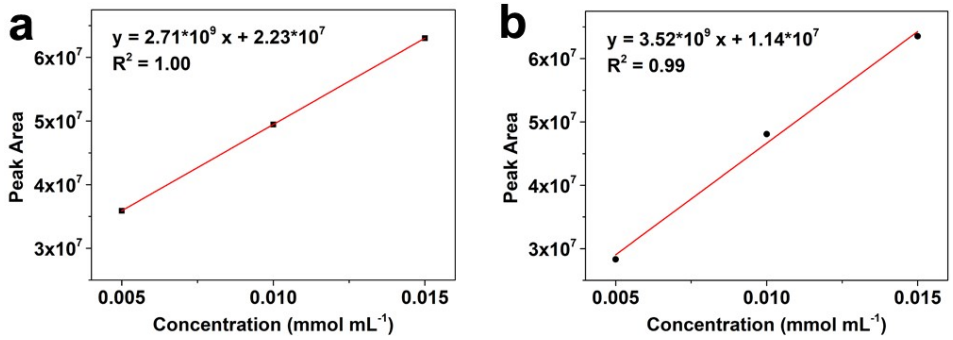

Fig. S20 Gas chromatograph spectrogram and the corresponding calibration curves of (a) benzaldehyde and (b) benzyl alcohol.

Table S1 Percentage of Mo and S atoms in different samples by XPS analysis.

Sample	atom% of Mo	atom% of S	Atom ratio of Mo/S
defective MoS_2/CFC	3.18	9.36	1:2.94
bulk MoS_2	18.25	36.68	1:2.01

Table S2 The detailed data of electrocatalytic hydrogenation of cinnamaldehyde (CAL) by the defective MoS_2/CFC.

Potential	Reaction time	Conversion	Selectivity (%)			FE	TOF
(V vs. RHE)	(h)	(%)	HCAL	COL	HCOL	(%)	(mmol $mmol_{MoS2}^{-1}$ h^{-1})
-0.2	5	52.3	22.0	70.6	7.4	100.0	7.5
-0.3	5	54.8	32.7	63.8	3.5	100.0	7.9
-0.4	5	60.7	34.8	62.6	2.6	95.9	8.7
-0.5	5	73.0	35.7	59.2	5.1	93.2	10.5
-0.6	5	81.6	45.1	51.7	3.2	91.3	11.7
-0.7	5	88.8	45.7	48.3	6.0	76.5	12.8
-0.8	5	83.0	47.2	28.2	24.6	55.1	11.9
-0.9	5	83.9	58.8	19.1	22.1	40.5	12.1

Table S3 The performance comparison of the defective MoS_2/CFC with the representative reports basing on electrocatalytic CAL selective hydrogenation.

Catalyst	Condition	Conversion (%)	Selectivity (%)			Reference
			HCAL	COL	HCOL	
defective MoS_2/CFC	-0.7 V vs. RHE, 5h	88.8	45.7	48.3	6.0	This work
Ta_2O_5/Ru-4.0-400	-1.1 V vs. RHE, 5h	69.8	100	/	/	[1]
RuO_2-SnO_2-TiO_2/Ti	-0.85 V vs. RHE, 5h	58.0	/	88.86	/	[2]
CoS_2 NCs	-0.9 V vs. RHE, 3.3h	90.6	91.7	/	/	[3]
CoS_{2-x} NCs	-0.9 V vs. RHE, 3.3h	92.1	/	/	93.0	[3]
Pt-10/C-0.2	0.05 A	12.0	2.5	6.0	1.0	[4]
GMP-Pd/NF	10 mA cm^{-2}, 6h	71.1	/	90.3	/	[5]
Pd/CF	50 mA cm^{-2}, 7h	96.21	19.52	57.88	8.14	[6]

Table S4 The detailed data of electrocatalytic hydrogenation of furfural (FAL) by the defective MoS_2/CFC.

Potential (V vs. RHE)	Reaction time (h)	Conversion (%)	Selectivity (%)	FE (%)	TOF (mmol $mmol_{MoS2}^{-1}$ h^{-1})
-0.2	5	25.1	100.0	60.1	3.6
-0.3	5	28.6	100.0	34.7	4.1
-0.4	5	36.8	100.0	24.7	5.3
-0.5	5	45.5	100.0	17.8	6.5
-0.6	5	47.2	100.0	20.8	6.8
-0.7	5	83.3	100.0	25.3	12
-0.8	5	92.6	100.0	12.4	13.3
-0.9	5	65.4	100.0	8.9	9.4

Table S5 The detailed data of electrocatalytic hydrogenation of benzaldehyde by the defective MoS_2/CFC.

Potential (V vs. RHE)	Reaction time (h)	Conversion (%)	Selectivity (%)	FE (%)	TOF (mmol $mmol_{MoS2}^{-1}$ h^{-1})
-0.3	5	18.5	100.0	24.7	2.7
-0.4	5	20	100.0	20.3	2.9
-0.5	5	27	100.0	11.4	3.9
-0.6	5	28.3	100.0	9.6	4.1
-0.7	5	29.4	100.0	13.4	4.2
-0.8	5	34.5	100.0	14.3	5.0
-0.9	5	66.7	100.0	9.4	9.6
-1.0	5	81.7	100.0	10.1	11.8

Reference

1. T. Wu, H. Meng and R. Dang, Amorphous Ta_2O_5-supported Ru as an efficient electrocatalyst for selective hydrogenation of cinnamaldehyde with water as the hydrogen source, *Inorg. Chem. Front.*, 2021, **8**, 4712-4719.
2. X. Huang, L. Zhang, C. Li, L. Tan and Z. Wei, High selective electrochemical hydrogenation of cinnamaldehyde to cinnamyl alcohol on RuO_2-SnO_2-TiO_2/Ti electrode, *ACS Catal.*, 2019, **9**, 11307-11316.
3. S. Han, Y. Shi, C. Wang, C. Liu and B. Zhang, Hollow cobalt sulfide nanocapsules for electrocatalytic selective transfer hydrogenation of cinnamaldehyde with water, *Cell Rep. Phys. Sci.*, 2021, **2**, 100337.
4. M. J. Torres, P. Sánchez, A. de Lucas-Consuegra and A. R. de la Osa, Electrocatalytic hydrogenation of cinnamaldehyde in a PEM cell: the role of sodium hydroxide and platinum loading, *Mol. Catal.*, 2020, **492**, 110936.
5. Y. Gao, A. Kong, M. Peng, Y. Lv, M. Liu, W. Li, J. Zhang and Y. Fu, Tuning electrochemical environment enables unexpected C=O selectivity for cinnamaldehyde hydrogenation over self-standing palladium cathode, *Mol. Catal.*, 2022, **529**, 112536.
6. H. Chen, T. Peng, B. Liang, D. Zhang, G. Lian, C. Yang, Y. Zhang and W. Zhao, Efficient electrocatalytic hydrogenation of cinnamaldehyde to value-added chemicals, *Green Chem.*, 2022, **24**, 3655-3661.